European Radiology (2019) 29:5852–5860
https://doi.org/10.1007/s00330-019-06113-y

MAGNETIC RESONANCE

Lesion detection performance of an abbreviated gadoxetic acid–enhanced MRI protocol for colorectal liver metastasis surveillance

Rodrigo Canellas[1] · Midhir J. Patel[1] · Sheela Agarwal[2,3] · Dushyant V. Sahani[1]

Received: 30 October 2018 / Revised: 7 February 2019 / Accepted: 14 February 2019 / Published online: 19 March 2019

Abstract

Objective To assess the lesion detection performance of an abbreviated MRI (AMRI-M) protocol consisting of ultrafast SE T2W, DWI, and T1W-HBP at 20 min for colorectal liver metastasis (CRLM) surveillance.

Methods In this Institutional Review Board (IRB)–approved retrospective study, gadoxetic acid–enhanced MRI scans of 57 patients (43 with pathologically proven CRLMs) were assessed. Two readers independently evaluated two sets of images per patient and commented on the number, location, and size of liver lesions. Set 1 included ultrafast spin-echo (SE) T2-weighted (T2W) + T1-weighted (T1W) hepatobiliary phase (HBP) at 20 min sequences + diffusion-weighted imaging (DWI), and set 2 consisted of the standard MRI protocol. A maximum of 10 lesions per patient were recorded. Cohen's kappa analysis, sensitivity, areas under the curve (AUCs), and the MRI cost analysis of the AMRI-M protocol were assessed.

Results Between 198 and 209 lesions were assessed with each set of images. The inter-observer agreement for the abbreviated protocol was reported excellent ($\kappa = 0.91$). The sensitivity and AUCs for the lesion characterization of AMRI-M protocol were very high (over 90%) for both readers. No statistically significant differences in sensitivity (assessed by mixed-effects logistic regression) and AUCs for lesion characterization (by ROC regression) were found between both protocols. The AMRI-M acquisition time was estimated to be less than 10 min, which translated into 59% cost of standard MRI.

Conclusion Our proposed AMRI-M protocol (ultrafast SE T2W, DWI, and T1W-HBP at 20 min) is fast, low-cost alternative to the standard MRI protocol and has a high lesion detection performance.

Key Points

- *Gadoxetic acid–enhanced protocol has increased the accuracy, sensitivity, and specificity of MRI for detecting colorectal liver metastases.*
- *Our proposed abbreviated MRI protocol is fast, low-cost alternative compared with the standard MRI protocol and has a high lesion detection performance.*
- *Adoption of our protocol may translate to substantial savings for patients and payers.*

Keywords Colorectal neoplasms · Liver · Gadolinium ethoxybenzyl DTPA · Magnetic resonance imaging

Abbreviations

AMRI-M	Abbreviated MRI
CE-MRI	Contrast-enhanced magnetic resonance imaging
CECT	Contrast-enhanced computed tomography
CRC	Colorectal cancer
CRLMs	Colorectal liver metastases
DWI	Diffusion-weighted imaging
HBP	Hepatobiliary phase
HCC	Hepatocellular carcinoma
IRB	Institutional Review Board
SE	Spin echo
T1W	T1-weighted
T2W	T2-weighted

✉ Rodrigo Canellas
rodcanellas@gmail.com

[1] Division of Abdominal Imaging and Interventional Radiology, Department of Radiology, Massachusetts General Hospital, White 270, 55 Fruit Street, Boston, MA 02114, USA

[2] Lenox Hill Radiology, New York City, NY, USA

[3] Bayer US LLC, Whippany, NJ, USA

Introduction

Imaging plays a pivotal role in the detection, management, and post-treatment surveillance of colorectal liver metastases (CRLMs). Accurate staging is required to stratify patients who would benefit from surgery, minimally invasive imaging-guided therapy, radiotherapy, and/or pharmaceutical treatment [1, 2].

Ultrasound and contrast-enhanced computed tomography (CECT) are historically first-line imaging tools for the assessment of metastatic liver lesions [3]. However, these modalities have a low sensitivity and specificity for the detection and particularly characterization of liver lesions. These limitations have paved the way for contrast-enhanced magnetic resonance imaging (CE-MRI), which has now become the modality of choice in triaging patients with suspected CRLMs [4, 5].

The introduction of hepatobiliary contrast media, gadoxetic acid, has further increased the accuracy, sensitivity, and specificity of MRI, which has an incremental value when combined with CECT for detecting additional liver metastases, especially in colorectal cancer (CRC) [6–9].

Nevertheless, MRI is still associated with long examination and interpretation times, which increases the costs and limits its routine use as a surveillance-imaging tool [10]. In order to make MRI more accessible, there has been an increasing interest in developing abbreviated MRI (AMRI) protocols, which have been successfully utilized in hepatocellular carcinoma (HCC) and prostate cancer screening [11–13]. The purpose of our study is to assess whether an AMRI-M protocol consisting of T1-weighted (T1W) hepatobiliary phase (HBP) at 20 min, ultrafast spin-echo (SE) T2-weighted (T2W) acquisition, and a diffusion-weighted imaging (DWI) has a similar lesion detection performance compared with standard gadoxetic acid–enhanced MRI protocol for CRLM surveillance.

Materials and methods

This retrospective study was approved by the Institutional Review Board (IRB), which waived the requirement for patient informed consent, and was conducted in accordance with the Health Insurance Portability and Accountability Act guidelines for research.

Patients

Patients with history of CRC who underwent MRI-based surveillance for liver metastases were included in the study. The inclusion criteria were as follows: patients with pathologically proven CRLMs who had undergone a standard gadoxetic acid–enhanced MRI of the abdomen (only one and the first MRI was included for each patient—index MRI). The exclusion criteria were patients who underwent surgery or ablative procedures prior to index MRI and patients who had no follow-up imaging studies (CECT, CE-MRI, and/or positron emission tomography-CT).

Initial electronic search in our database for pathology reports containing the words "hepatectomy," "liver biopsy," and "colorectal cancer" resulted in a total of 136 entries between January 2011 and July 2017. From this initial cohort, all patients who had not undergone gadoxetic acid–enhanced MRI were excluded ($n = 74$). Furthermore, all patients with more than 10 liver lesions ($n = 12$) and who underwent invasive treatment prior to the index MRI were also excluded ($n = 7$). Patients who had undergone a standard gadoxetic acid–enhanced MRI of the abdomen (regardless of the primary tumor) and did not have any liver lesion formed our control group. These patients were not subjected to inclusion or exclusion criteria.

A total of 43 patients (mean age 53 years ± 13.2) with colorectal liver metastases and 14 patients (mean age 53 years ± 18.3) without identifiable colorectal liver metastases formed the final cohort. A flowchart showing patient selection is provided in Fig. 1.

MRI technique

All patients underwent dynamic CE-MRI of the abdomen performed on a 1.5-T ($n = 45$; Signa HDxt GE Medical Systems and Magnetom Avanto, Siemens Healthcare) or 3.0-T ($n = 12$; Discovery 750MR GE Medical Systems and Magnetom Trio, Siemens Healthcare) scanners. Patients were positioned supine with a phased array receiver coil covering the upper abdomen. The T2W sequences included a breath-hold coronal ultrafast SE and an axial fast spin echo (FSE) with fat saturation. T1W in-phase and out-of-phase sequences were also included. DWI was acquired with b values ranging from 0 to 1000 s/mm^2. ADC maps were generated by a mono-exponential function using b values ranging from 0 to 1000 s/mm^2. The axial T2W and DWI sequences were acquired post-contrast. The dynamic contrast-enhanced images were obtained with gadoxetic acid (Primovist®, Bayer Healthcare Pharmaceuticals) using T1W fat-suppressed sequences: precontrast, arterial-phase (25–35 s), portal-phase (60 s), late-phase (3 min), early hepatobiliary phase (5–8 min), and delayed hepatobiliary phase (15–20 min) images. A total contrast volume of 10 ml was administered intravenously by automatic power injector at a rate of 1 ml/s followed by 20 ml saline flush. The image acquisition protocol is summarized in Tables 1 and 2. The scan acquisition time for our standard gadoxetic acid–enhanced MRI protocol ranged from 35 to 45 min. Considering ultrafast SE T2W sequence takes around 30 s, DWI around 4 min, and T1W-HBP (axial and coronal) around 1 min to be completed, the proposed AMRI-M protocol has an estimated scanner time of less than 10 min, assuming patients will be manually injected outside the

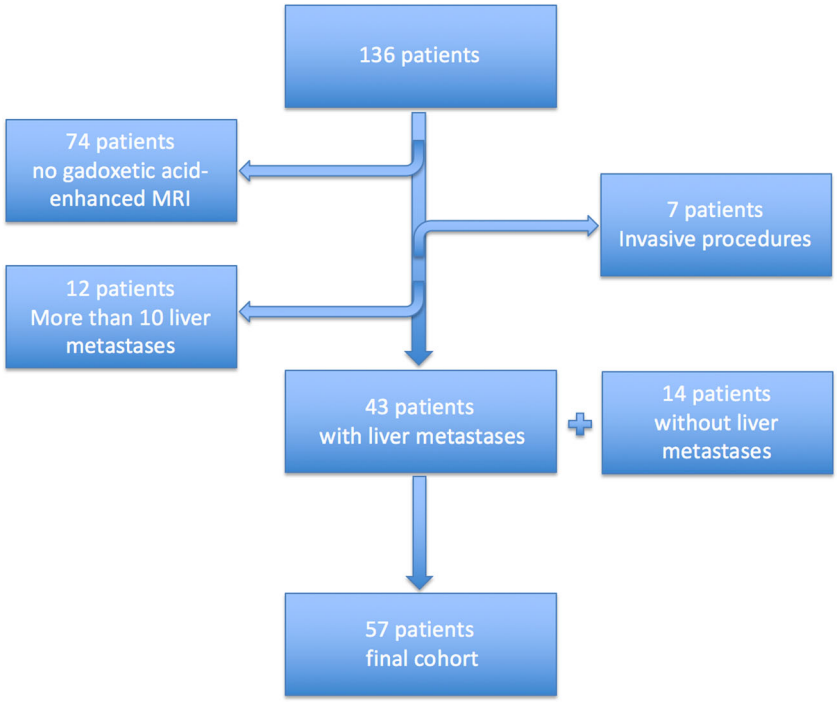

Fig. 1 Flowchart shows derivation of study cohort

scanner room and all sequences will be acquired approximately 20 min after the injection of contrast. If the time required for patient setup (around 5 min) had been added to the scanner time, the time spent by a patient in the scanner room would have been less than 15 min. In order to optimize MRI workflow and eliminate delays associated with gadoxetic acid contrast uptake, a flowchart is provided in Fig. 2.

Current literature supports that T2W and DWI sequences can be acquired after the injection of gadoxetic acid without significant changes in lesion detectability [14].

Image analysis

Two radiologists (RC and MP, with 9 and 6 years of experience in abdominal imaging interpretation, respectively) independently reviewed all images on a PACS workstation (Impax 4.0; Agfa). Both readers were aware of patient's diagnosis (cancer) but were blinded to all other clinical information.

In order to simulate an AMRI protocol, each reader independently reviewed two sets of sequences per patient. The first set included T1W-HBP at 15–20 min (coronal and axial planes), ultrafast SE T2W (coronal plane) sequences, and DWI. The second set of images, including all sequences of the standard gadoxetic acid–enhanced MRI protocol, was assessed 4 weeks after the assessment of the first set in order to eliminate any recall bias.

Even though we decided to use delayed T1W-HBP at 15–20 min in the imaging sets as opposed to T1W-HBP at 10 min, recent literature has suggested that the latter can have a similar detection capability for CRLMs [15–17]. Nevertheless, the scan acquisition time would not be affected by any of them.

Table 1 MRI acquisition parameters

Sequence	TR/TE	Flip angle (°)	Section thickness (mm)	Field of view (mm)	Matrix
T1-weighted 3D	3.27/1.19	25	3.5	300 × 400	256 × 154
T1-weighted in-phase (GRE)	8.232/4.168	12	5.0	400	320 × 192
T1-weighted out-of-phase (GRE)	8.232/2.084	12	5.0	400	320 × 192
Balanced GE T2-weighted	3706/1.6	45	6.0	440	320 × 256
FSE T2-weighted with fat saturation	6316/113.5	90	5.0	420	512 × 256
Ultrafast SE T2-weighted	1178/141	90	6.0	440	384 × 192
DWI (B50, B400, B800)	6000/60	90	6.0	296 × 379	192 × 120

GRE, gradient echo; *FSE*, fast spin echo; *DWI*, diffusion-weighted imaging; *TR*, repetition time; *TE*, echo time

Table 2 Sequences included in both protocols

	Standard MRI protocol	Abbreviated MRI protocol
Ultrafast SE T2-weighted (coronal)	✓	✓
Balanced GE T2-weighted (coronal)	✓	✗
Fast SE w/ fat saturation T2-weighted (axial)	✓	✗
DWI (B0-B1000; axial)	✓	✓
GRE T1-weighted in-phase and out-of-phase (axial)	✓	✗
3D T1-weighted w/ fat saturation precontrast, 25–35 s, 70 s, 3 min, 5–10 min post-contrast (axial)	✓	✗
3D T1-weighted w/ fat saturation 15–20 min post-contrast (axial and coronal)	✓	✓
Acquisition time	35–50 min	< 10 min

GE and *GRE*, gradient echo; *FSE*, fast spin echo; *DWI*, diffusion-weighted imaging

Due to improvements in image quality of DWI [18] and its higher sensitivity for the detection of liver metastases, the low *b* values can serve as a replacement for FSE T2W sequence. This is well supported by the published literature [19, 20], and there has been an increasing clinical adoption of this practice. This is one of the reasons we decided not including FSE T2W sequence in our abbreviated protocol. Moreover, ultrafast T2W sequence can assess the characterization of cysts and hemangiomas, and the high *b* values of DWI can help characterizing solid lesions.

Although we included ultrafast T2W and DWI sequences in our AMRI-M, one should be free to include FSE T2W sequence over ultrafast T2W sequence (at the cost of increased MRI acquisition time) for a similar abbreviated protocol.

Lesion detection

Each reader recorded the number of all liver lesions, segmental location (Couinaud classification of hepatic segments) with corresponding slice number, and lesion size (largest diameter) for up to 10 lesions on the first and second set of images. All lesions were individually annotated.

Lesion characterization

Both readers also characterized each lesion as malignant (metastatic lesion) or benign (cysts, hemangiomas, adenomas, or focal nodular hyperplasia).

As fewer sequences were included on the AMRI-M protocol, we decided to assess whether our protocol would be able to differentiate malignant from benign lesions rather than try to provide a definitive diagnosis for each lesion.

A malignant lesion was diagnosed on AMRI-M as follows: (1) when a hypointense lesion on T1W-HBP at 20 min showed restricted diffusion on DWI images and/or (2) when a hypointense lesion on T1W-HBP at 20 min showed a signal intensity different from cysts/hemangiomas on ultrafast SE T2W sequence (Figs. 3 and 4).

Reference standard

All patients, with the exception of control group, had a pathologically proven metastatic disease by means of percutaneous biopsy ($n = 19$) or liver resection ($n = 24$). For all lesions without histopathological examination, the standard gadoxetic acid–enhanced MRI protocol and all available follow-up studies (CECT, CE-MRI, and/or positron emission tomography-CT) were used to provide the correct number of liver lesions and to accurately characterize them as malignant or benign.

The median time and interquartile range between the index MRI and the follow-up studies were 70 and 72 days, respectively.

MRI cost analysis

Based on 2017 Medicare reimbursement (Healthcare Common Procedure Coding System [HCPCS] codes 74182), the total cost of standard CE-MRI was assessed with breakdown of technical and professional components. The cost of AMRI-M was estimated by keeping constant the cost of professional component and reducing by half the cost of technical component (which was conservatively assumed to be half of standard CE-MRI). A similar approach to estimate the cost of an AMRI protocol for HCC detection has been recently published [12].

The number of follow-up studies (MRI of the abdomen) was also assessed for each patient in our cohort. The mean number of follow-up imaging studies and the estimated cost savings were assessed, assuming that all patients had undergone AMRI-M protocol for surveillance.

Statistical analysis

Continuous variables were presented as mean ± standard deviation (SD). Intra- and inter-observer agreements between the readers were assessed with Cohen's kappa statistics. A kappa ≤ 0.20 was regarded as poor, 0.21–0.40 fair, 0.41–0.60

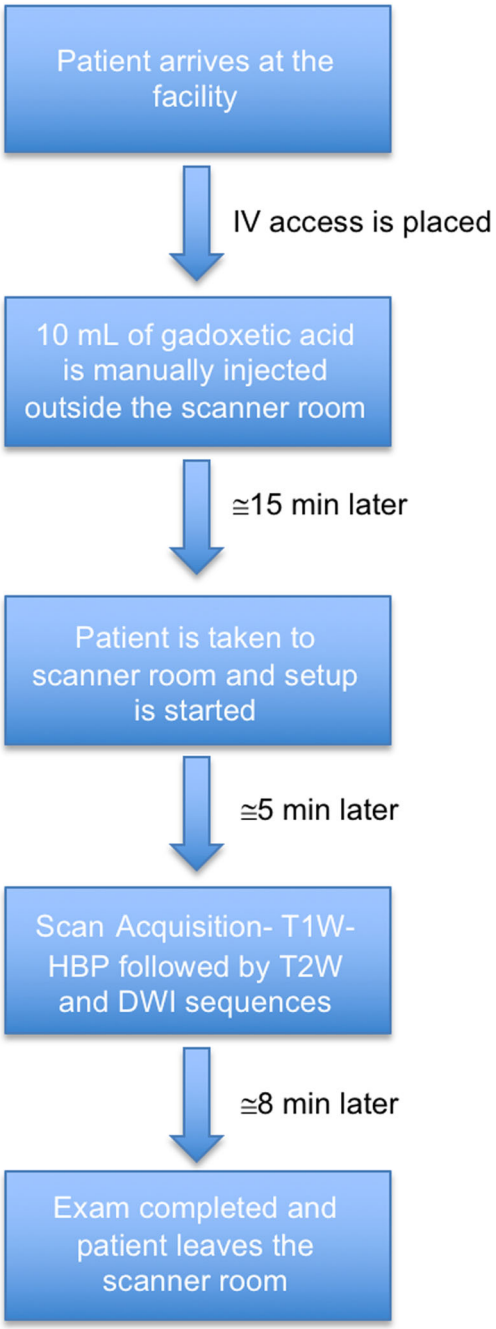

Fig. 2 Flowchart shows an optimized workflow for the AMRI-M protocol

moderate, 0.61–0.80 good, and > 0.80 excellent agreement [21]. The sensitivity of the AMRI-M was obtained for each reader. The cost of the MRI examinations was also estimated.

Ninety-five percent confidence intervals (95% CI) were used for statistical inference and adjusted for clustering [22]. Differences in sensitivities between both protocols were assessed by mixed-effects logistic regression. Areas under the curve (AUCs)—and their differences—were constructed for the assessment of lesion characterization using a nonparametric analysis of clustered data (receiver operating characteristic regression).

All statistical analyses were performed using SPSS (version 25.0, IBM Corp.) and STATA (version 15.1, StataCorp). P values < 0.05 were considered to indicate statistical significance.

Results

Lesion detection

A total of 57 patients were included in the study, 28 males (54 years ± 13.3) and 29 females (54 years ± 15.8). Patient demographics are summarized in Table 3. Between 198 and 209 lesions were assessed by each reader per protocol. The mean lesion size was 18 ± 12 mm.

The standard MRI protocol detected 210 liver lesions. Reader 1 detected 198 lesions on the AMRI-M protocol and 198 lesions on standard protocol. Reader 2 detected 202 lesions on AMRI-M protocol and 209 lesions on standard protocol. No false positive lesions were detected on the control group.

Intra- and inter-observer assessment

The intra-observer agreement was reported excellent for both readers ($\kappa = 0.91$ and $\kappa = 0.92$) along with the inter-observer agreement for the abbreviated protocol ($\kappa = 0.91$). Amongst lesions in which there was no agreement, 75% (12/16) measured less than 10 mm.

Lesion characterization

The standard MRI protocol detected 210 liver lesions (169 malignant, 37 benign, and 4 indeterminate); 108/210 (51.4%) were greater than 10 mm, of which the vast majority was malignant (103/108). One hundred two out of 210 lesions were less than or equal to 10 mm; the majority was also malignant (68/102). Amongst the indeterminate lesions, all of them measured less than 10 mm. The reference standard helped characterizing them as 2 malignant and 2 benign lesions. However, for the assessment of the AUCs, these 4 lesions were removed from the AMRI-M analysis and considered missed diagnosis for the standard protocol analysis. On per lesion basis, the sensitivity of standard MRI protocol was 100% (95% CI [1.00–1.00]).

Reader 1 detected 198 lesions on the AMRI-M protocol (165 malignant and 30 benign); 3 of them represented partial volume artifact (false positives). On per lesion basis, the sensitivity was 92.8% (95% CI [0.88–0.95]). For lesions greater than 10 mm, reader 1 detected all and accurately characterized 104 out of 108. For lesions less than or equal to 10 mm, reader 1 detected 87/102 and correctly characterized 81 out of 85 (2 indeterminate lesions).

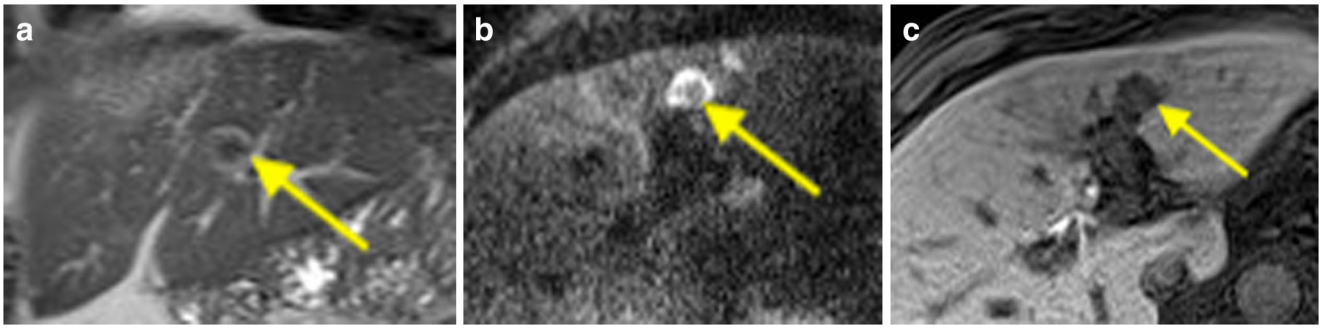

Fig. 3 A 56-year-old male with metastatic colorectal cancer. **a** Coronal ultrafast SE T2W sequence shows a hypointense lesion in the liver segment II/III (arrow). **b** Axial DWI ($b = 800$) and **c** axial T1W-HBP at 20 min show the same lesion. Given the signal intensity on T2W (hypointense) and DWI (hyperintense), both readers characterized this lesion as malignant

Reader 2 detected 202 lesions on the AMRI-M protocol (163 malignant and 35 benign); 4 of them represented partial volume artifact (false positives). On per lesion basis, the sensitivity was 94.2% (95% CI [0.89–0.97]). Amongst lesions greater than 10 mm, reader 2 detected 106 lesions and correctly characterized 105 of them. For lesions less than or equal to 10 mm, reader 2 detected 92/102 and correctly characterized 85 out of 90 (2 indeterminate lesions).

After removing the indeterminate lesions, the lesions missed by each reader, and the false positive lesions, the area under the curve (AUC) of the AMRI-M protocol to characterize all detected and true liver lesions (regardless the size) was 90.7% (95% CI [0.72–0.99]) for reader 1 ($n = 193$) and 94.6% (95% CI [0.86–0.99]) for reader 2 ($n = 196$). The AUC of the standard MRI protocol was 96.8% (95% CI [0.90–1.00]).

We could not find evidence of statistically significant differences between the sensitivities of the AMRI-M and the full standard MRI protocol ($p > 0.05$). Moreover, no statistically significant differences were found between the AUCs of both readers ($p = 0.27$), between reader 1 and standard MRI protocol ($p = 0.22$), and between reader 2 and standard MRI protocol ($p = 0.10$). Table 4 shows the results of the readers' analysis.

The mean per patient sensitivity was estimated to be 93.7% (95% CI [0.90–0.97]) for reader 1 and 95.2% (95% CI [0.92–0.98]) for reader 2.

Estimated cost savings

The total cost of the standard CE-MRI protocol was fixed to be $528.70 based on 2017 Medicare reimbursement, respectively. The costs of the professional and technical were $93.97 and $434.73, respectively.

The estimated cost of the AMRI-M protocol was $311.33 (434.73/2 + 93.97), which represents 59% of the standard CE-MRI.

The mean number of follow-up studies per patient with colorectal liver metastases was ≅ 5 MRIs ± s4. If the patients had undergone AMRI-M protocol instead of standard CE-MRI, the estimated mean cost savings would have been $1.083.83 (5 MRIs × 528.70 × 41/100) per patient. Now considering that all patients had undergone AMRI-M protocol for the follow-up studies instead of the standard CE-MRIs ($n = 201$), the estimated total cost savings would have been $43.570.17 (201 MRIs × $528.70 × 41/100) in our cohort group.

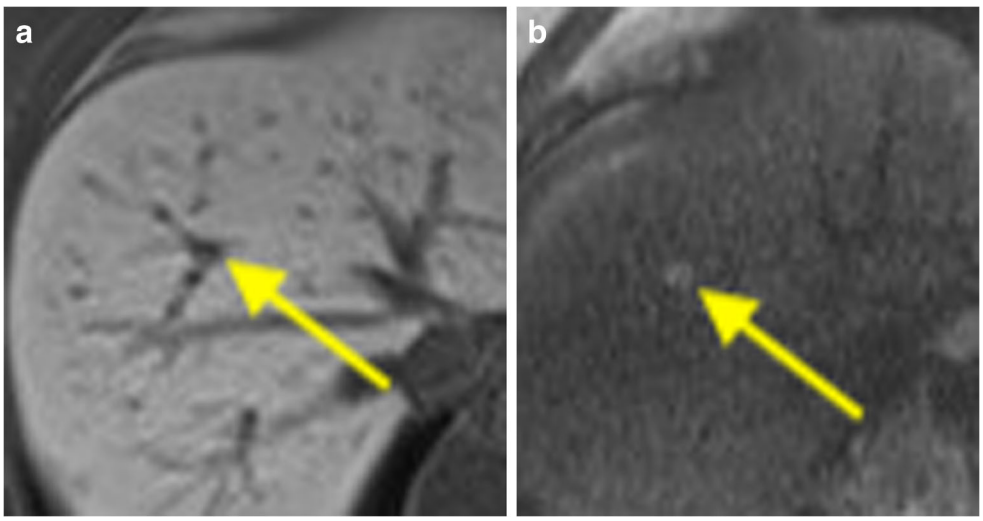

Fig. 4 A 57-year-old male with metastatic colorectal cancer.(**a**) Axial T1W-HBP at 20 min shows a subcentimeter metastatic lesion (arrow) in the liver segment VIII. Both readers missed it on this sequence given the small size and the proximity to liver vessels. However, it was easily appreciated on (**b**) DWI

Table 3 Demographics and clinical information of study cohort

Number of patients	57
Gender (M/F)	28 (49%)/29 (51%)
Age (mean + SD) in years	54 ± 14.5
Number of patients with CRC	43
Gender (M/F) with CRC	23 (53%)/20 (47%)
Age (mean + SD) in years with CRC	53 ± 13.2
Number of patients in the control group	14
Gender (M/F) in the control group	5 (36%)/9 (64%)
Age (mean + SD) in years in the control group	53 ± 18.3
Histopathology (biopsy/hepatectomy) with CRC	19 (44%) / 24 (56%)
Chemotherapy prior to MRI with CRC	14/43 (32%)
Number of lesions per patient with CRC (mean + SD)	4.9 ± 2.7
Lesion size (mean + SD) in mm	18.5 ± 12

M, male; *F*, female; *SD*, standard deviation; *CRC*, colorectal cancer

Discussion

The results of our study showed that our proposed AMRI-M protocol (T1W-HBP at 20 min [coronal and axial planes], ultrafast SE T2W sequence [coronal plane], and DWI [axial plane]) had a high lesion detection performance for CRLMs. An excellent agreement between the readers, high sensitivity, and AUCs (all over 90%) were reported. It is worthy to mention that, in retrospect, all lesions missed on the AMRI-M protocol were picked up on at least one of the abovementioned sequences.

Ultrafast T2W sequence was useful for the characterization of cysts and hemangiomas. DWI was useful for characterizing malignant lesions and also in detecting small lesions adjacent to liver vessels. Moreover, DWI can help detecting extrahepatic metastases of colorectal cancer in the abdomen and pelvis [23–26]. Both readers also pointed out that coronal T1W-HBP images were useful for evaluating small peripheral lesions and for differentiating them from partial volume averaging. Considering the estimated scan acquisition time of the AMRI-M is approximately 8 min and factoring patient setup time of approximately 5 min, the entire exam can conceivably be accomplished under 15 min. This amount of time is less than one third of the time it takes for the standard gadoxetic acid–enhanced MRI protocol. Thus, for a 45-min time slot (usually set for a single standard CE-MRI of the abdomen), it would be possible to perform about three patient scans using the AMRI-M protocol.

Even though the AMRI-M protocol is highly sensitive and accurate for the characterization of liver lesions, our results reflect just a preliminary experience and we would not recommend using it as the initial staging exam, where lesion characterization is paramount (especially for subcentimeter lesions, which diagnosis can be challenging even for the standard MRI protocol) [27, 28]. Therefore, a prior standard CE-MRI study would be required to characterize all preexisting lesions. Moreover, this protocol should be used for surveillance in the outpatient setting and for patients with advanced disease (not candidates for curative resection of liver metastases). Patients experiencing abdominal pain, fever, jaundice, or any other acute symptoms should undergo the standard CE-MRI protocol.

In our study, it was also demonstrated that the cost of the standard gadoxetic acid–enhanced MRI protocol can potentially be reduced by ≅ 40% by utilizing our AMRI-M protocol, without compromising diagnostic information. The total cost savings (adopting the AMRI-M protocol as opposed to standard protocol) were estimated at $43.570.17 in our small cohort. Considering that advanced treatment options have dramatically improved the overall survival of patients with CRLMs [29, 30], adoption of our protocol may translate to substantial savings for patients and payers.

Our results are in accordance with the recently published literature. In a meta-analysis compelling 39 articles, Vilgrain et al [31] reported a sensitivity of 90.6% and 95.5% (95% CI [0.93–0.96], 28 datasets) for the gadoxetic acid–enhanced MRI protocol alone and combined with DWI, respectively, for the

Table 4 Results of readers' analysis

	Reader 1	Reader 2	*p* values*	
Number of lesions detected, abbreviated protocol	198 (3 false positives)	202 (4 false positives)	–	
Number of lesions detected, reference standard	210		–	
Inter-observer agreement, abbreviated protocol	0.91		–	
Sensitivity, abbreviated protocol (detection)	92.8%	94.2%	0.054**	
Sensitivity, standard protocol	100%		0.08** (reader 1)	0.15** (reader 2)
AUCs, abbreviated protocol (characterization)	0.91	0.95	0.27***	
AUCs, standard protocol (characterization)	0.97		0.22*** (reader 1)	0.10*** (reader 2)

AUCs, areas under the curve

**p* values represent differences between reader 1 and reader 2 and between reader 1 and reader 2 vs reference standard

***p* values assessed by mixed-effects logistic regression

****p* values assessed by receiver operating characteristic (ROC) regression

detection of liver metastases. Marks et al [32] demonstrated that an AMRI protocol consisting of ultrafast SE T2W and T1W-HBP sequences has a high negative predictive value and may be an acceptable method for hepatocellular carcinoma (HCC) surveillance. Tillman et al [33] reported that a similar AMRI protocol provides higher per-lesion sensitivity and negative predictive value than ultrasound for HCC screening. Besa et al [12] estimated the cost of an AMRI protocol, including DWI and T1W-HBP sequences, to be 30–35% of the standard CE-MRI cost. The concepts of AMRI have also been explored by Cunha et al [34], who demonstrated that a protocol consisting of liver fat and iron quantification, MR elastography, and visceral adipose tissue is a feasible, less-costly, and accessible option for screening and monitoring patients with obesity, nonalcoholic fat liver disease, and metabolic syndrome.

Our study has several limitations. This was a retrospective study with a small cohort; therefore, the reported findings reflect just a preliminary experience of the AMRI-M protocol. Further prospective studies in larger cohorts are necessary to confirm our findings. Secondly, not every lesion included in our study was histopathologically proven. Nevertheless, in the course of patients with liver metastases (especially those with unresectable disease), most lesions will not need biopsy and the diagnosis will rely on imaging findings. Given the retrospective nature of our study, the true acquisition time of the AMRI-M protocol is not known. Moreover, only one site of metastatic disease was assessed in our analysis (liver). However, DWI is a reliable tool to detect bone lesions, lymphadenopathy, and peritoneal disease [35–37], and we believe that the assessment of these sites will not be compromised by using the AMRI-M protocol. Regarding lesion characterization, the results of our study might have been overestimated due to high prevalence of malignant lesions. However, in clinical practice, when an MRI is requested to stage these patients, a history of primary tumor is usually given and a positive CT study for liver lesions had already been performed (which also increases the prevalence of malignant lesions). Finally, the cost analysis of this study was based on several assumptions previously published; therefore, the real cost of the AMRI-M protocol in clinical practice is not yet established.

In conclusion, our proposed AMRI-M protocol had an excellent lesion detection and characterization performance in our patient cohort and has the potential to become an acceptable lower cost alternative to the standard gadoxetic acid–enhanced MRI protocol for CRLM surveillance. Moreover, it can significantly decrease MRI acquisition time and improve the efficiency of MRI workflow without compromising the diagnostic impact.

Acknowledgements We would like to acknowledge Harvard Catalyst's support for the revised version of the manuscript.

Funding This study has received funding by Bayer US.

Compliance with ethical standards

Guarantor The scientific guarantor of this publication is Dushyant V. Sahani.

Conflict of interest One of the authors of this manuscript declares relationships with the following companies: Bayer US. The other authors of this manuscript declare no relationships with any companies, whose products or services may be related to the subject matter of the article.

Statistics and biometry Some complex statistical methods were necessary for this paper.

Informed consent Written informed consent was waived by the Institutional Review Board.

Ethical approval Institutional Review Board approval was obtained.

Methodology
- retrospective
- experimental
- performed at one institution

References

1. Niekel MC, Bipat S, Stoker J (2010) Diagnostic imaging of colorectal liver metastases with CT, MR imaging, FDG PET, and/or FDG PET/CT: a meta-analysis of prospective studies including patients who have not previously undergone treatment. Radiology 257:674–684
2. Frankel TL, Gian RK, Jarnagin WR (2012) Preoperative imaging for hepatic resection of colorectal cancer metastasis. J Gastrointest Oncol 3:11–18
3. Tirumani SH, Kim KW, Nishino M et al (2014) Update on the role of imaging in management of metastatic colorectal cancer. Radiographics 34:1908–1928
4. Schulz A, Viktil E, Godt JC et al (2016) Diagnostic performance of CT, MRI and PET/CT in patients with suspected colorectal liver metastases: the superiority of MRI. Acta Radiol 57:1040–1048
5. Ko Y, Kim J, Park JK et al (2017) Limited detection of small (</= 10 mm) colorectal liver metastasis at preoperative CT in patients undergoing liver resection. PLoS One 12:e0189797
6. Kim HJ, Lee SS, Byun JH et al (2015) Incremental value of liver MR imaging in patients with potentially curable colorectal hepatic metastasis detected at CT: a prospective comparison of diffusion-weighted imaging, gadoxetic acid-enhanced MR imaging, and a combination of both MR techniques. Radiology 274:712–722
7. Scharitzer M, Ba-Ssalamah A, Ringl H et al (2013) Preoperative evaluation of colorectal liver metastases: comparison between gadoxetic acid-enhanced 3.0-T MRI and contrast-enhanced MDCT with histopathological correlation. Eur Radiol 23:2187–2196
8. Choi SH, Kim SY, Park SH et al (2017) Diagnostic performance of CT, gadoxetate disodium-enhanced MRI, and PET/CT for the diagnosis of colorectal liver metastasis: systematic review and meta-analysis. J Magn Reson Imaging. https://doi.org/10.1002/jmri.25852
9. Sofue K, Tsurusaki M, Murakami T et al (2014) Does Gadoxetic acid-enhanced 3.0T MRI in addition to 64-detector-row contrast-enhanced CT provide better diagnostic performance and change the therapeutic strategy for the preoperative evaluation of colorectal liver metastases? Eur Radiol 24:2532–2539

10. Zech CJ, Justo N, Lang A et al (2016) Cost evaluation of gadoxetic acid-enhanced magnetic resonance imaging in the diagnosis of colorectal-cancer metastasis in the liver: results from the VALUE Trial. Eur Radiol 26:4121–4130
11. Romeo V, Cuocolo R, Liuzzi R et al (2017) Preliminary results of a simplified breast MRI protocol to characterize breast lesions: comparison with a full diagnostic protocol and a review of the current literature. Acad Radiol 24:1387–1394
12. Besa C, Lewis S, Pandharipande PV et al (2017) Hepatocellular carcinoma detection: diagnostic performance of a simulated abbreviated MRI protocol combining diffusion-weighted and T1-weighted imaging at the delayed phase post gadoxetic acid. Abdom Radiol (NY) 42:179–190
13. Weiss J, Martirosian P, Notohamiprodjo M et al (2017) Implementation of a 5-minute magnetic resonance imaging screening protocol for prostate cancer in men with elevated prostate-specific antigen before biopsy. Invest Radiol. https://doi.org/10.1097/RLI.0000000000000427
14. Muhi A, Ichikawa T, Motosugi U, Sou H, Sano K, Araki T (2012) Diffusion- and T_2-weighted MR imaging of the liver: effect of intravenous administration of gadoxetic acid disodium. Magn Reson Med Sci 11:185–191
15. Lee D, Cho ES, Kim DJ, Kim JH, Yu JS, Chung JJ (2015) Validation of 10-minute delayed hepatocyte phase imaging with 30 degrees flip angle in gadoxetic acid-enhanced MRI for the detection of liver metastasis. PLoS One 10:e0139863
16. Sofue K, Tsurusaki M, Tokue H, Arai Y, Sugimura K (2011) Gd-EOB-DTPA-enhanced 3.0 T MR imaging: quantitative and qualitative comparison of hepatocyte-phase images obtained 10 min and 20 min after injection for the detection of liver metastases from colorectal carcinoma. Eur Radiol 21:2336–2343
17. van Kessel CS, Veldhuis WB, van den Bosch MA, van Leeuwen MS (2012) MR liver imaging with Gd-EOB-DTPA: a delay time of 10 minutes is sufficient for lesion characterisation. Eur Radiol 22:2153–2160
18. Rosenkrantz AB, Oei M, Babb JS, Niver BE, Taouli B (2011) Diffusion-weighted imaging of the abdomen at 3.0 tesla: image quality and apparent diffusion coefficient reproducibility compared with 1.5 tesla. J Magn Reson Imaging 33:128–135
19. d'Assignies G, Fina P, Bruno O et al (2013) High sensitivity of diffusion-weighted MR imaging for the detection of liver metastases from neuroendocrine tumors: comparison with T2-weighted and dynamic gadolinium-enhanced MR imaging. Radiology 268:390–399
20. Soyer P, Boudiaf M, Place V et al (2011) Preoperative detection of hepatic metastases: comparison of diffusion-weighted, T2-weighted fast spin echo and gadolinium-enhanced MR imaging using surgical and histopathologic findings as standard of reference. Eur J Radiol 80:245–252
21. Landis JR, Koch GG (1977) The measurement of observer agreement for categorical data. Biometrics 33:159–174
22. Genders TS, Spronk S, Stijnen T, Steyerberg EW, Lesaffre E, Hunink MG (2012) Methods for calculating sensitivity and specificity of clustered data: a tutorial. Radiology 265:910–916
23. Zhang H, Dai W, Fu C et al (2018) Diagnostic value of whole-body MRI with diffusion-weighted sequence for detection of peritoneal metastases in colorectal malignancy. Cancer Biol Med 15:165–170
24. Ogawa M, Ichiba N, Watanabe M, Yanaga K (2016) The usefulness of diffusion MRI in detection of lymph node metastases of colorectal cancer. Anticancer Res 36:815–819
25. Shinya S, Sasaki T, Nakagawa Y, Guiquing Z, Yamamoto F, Yamashita Y (2009) The efficacy of diffusion-weighted imaging for the detection of colorectal cancer. Hepatogastroenterology 56:128–132
26. Cho EY, Kim SH, Yoon JH et al (2013) Apparent diffusion coefficient for discriminating metastatic from non-metastatic lymph nodes in primary rectal cancer. Eur J Radiol 82:e662–e668
27. Goshima S, Kanematsu M, Watanabe H et al (2010) Hepatic hemangioma and metastasis: differentiation with gadoxetate disodium-enhanced 3-T MRI. AJR Am J Roentgenol 195:941–946
28. Doo KW, Lee CH, Choi JW, Lee J, Kim KA, Park CM (2009) "Pseudo washout" sign in high-flow hepatic hemangioma on gadoxetic acid contrast-enhanced MRI mimicking hypervascular tumor. AJR Am J Roentgenol 193:W490–W496
29. Cremolini C, Loupakis F, Antoniotti C et al (2015) FOLFOXIRI plus bevacizumab versus FOLFIRI plus bevacizumab as first-line treatment of patients with metastatic colorectal cancer: updated overall survival and molecular subgroup analyses of the open-label, phase 3 TRIBE study. Lancet Oncol 16:1306–1315
30. Gruenberger T, Bridgewater J, Chau I et al (2015) Bevacizumab plus mFOLFOX-6 or FOLFOXIRI in patients with initially unresectable liver metastases from colorectal cancer: the OLIVIA multinational randomised phase II trial. Ann Oncol 26:702–708
31. Vilgrain V, Esvan M, Ronot M, Caumont-Prim A, Aube C, Chatellier G (2016) A meta-analysis of diffusion-weighted and gadoxetic acid-enhanced MR imaging for the detection of liver metastases. Eur Radiol 26:4595–4615
32. Marks RM, Ryan A, Heba ER et al (2015) Diagnostic per-patient accuracy of an abbreviated hepatobiliary phase gadoxetic acid-enhanced MRI for hepatocellular carcinoma surveillance. AJR Am J Roentgenol 204:527–535
33. Tillman BG, Gorman JD, Hru JM et al (2017) Diagnostic per-lesion performance of a simulated gadoxetate disodium-enhanced abbreviated MRI protocol for hepatocellular carcinoma screening. Clin Radiol. https://doi.org/10.1016/j.crad.2017.11.013
34. Cunha GM, Villela-Nogueira CA, Bergman A, Lobo Lopes FPP (2018) Abbreviated mpMRI protocol for diffuse liver disease: a practical approach for evaluation and follow-up of NAFLD. Abdom Radiol (NY). https://doi.org/10.1007/s00261-018-1504-5
35. Fehniger J, Thomas S, Lengyel E et al (2016) A prospective study evaluating diffusion weighted magnetic resonance imaging (DW-MRI) in the detection of peritoneal carcinomatosis in suspected gynecologic malignancies. Gynecol Oncol 142:169–175
36. Goudarzi B, Kishimoto R, Komatsu S et al (2010) Detection of bone metastases using diffusion weighted magnetic resonance imaging: comparison with (11)C-methionine PET and bone scintigraphy. Magn Reson Imaging 28:372–379
37. Heijnen LA, Lambregts DM, Mondal D et al (2013) Diffusion-weighted MR imaging in primary rectal cancer staging demonstrates but does not characterise lymph nodes. Eur Radiol 23:3354–3360